Study of fatigue crack–hole interaction and prediction of crack path

A Thesis submitted in partial fulfilment of the requirements for the degree of

Master of Technology (Research)

by

Ajit Kumar

(Roll Number-612MM1003)

Under the supervision of

Prof. B. B. Verma (MM)

Prof. P. K. Ray (ME)

National Institute of Technology
Rourkela-769008

Department of Metallurgical and Materials Engineering

National Institute of Technology, Rourkela

India

July 2015

Department of Metallurgical and Materials Engineering
National Institute of Technology Rourkela,

India

CERTIFICATE

This is to certify that the thesis entitled "**Study of fatigue crack-hole interaction and prediction of crack path**" being submitted by **Mr. Ajit Kumar** to the National Institute of Technology Rourkela, for the award of the degree of **Masters of Technology (Research)** is a record of bonafide research work carried out under our supervision and guidance. The results presented in this thesis have not been submitted elsewhere for the award of any other degree or diploma. This work in our opinion has reached the standard of fulfilling the requirements for the award of the degree of **Masters of Technology (Research)** in accordance with the regulations of institute.

Prof. P. K. Ray

(Supervisor)

Date:

Prof. B. B. Verma

(Supervisor)

Acknowledgement

It is a privilege for me to express my profound gratitude and indebtedness to my supervisors **Prof. B. B. Verma,** Metallurgical & Materials Engineering Department, National Institute of Technology Rourkela and **Prof**. **P. K. Ray,** Mechanical Engineering Department, National Institute of Technology Rourkela. Without their efforts and guidance this work could not have been possible. They have guided me at all stages during this research work. I would like to convey my sincere gratitude to Head of the Department Prof. S. C. Mishra and my master scrutiny committee members, Prof. S. K. Sahu (ME) and Prof. S. Sen (MM) for assessing my research work and providing me valuable suggestions throughout the work**.**

I am also thankful to Mr. Rajesh Patnaik, and Mr. S. Hembram of NIT Rourkela for their technical guidance in conducting various experimental studies during the research work. I am also thankful to my seniors and friends Vaneshwar Sahoo, Lailesh Kumar and S. V. Abhinay for their help and support during my research work.

Special thanks to my parents for motivating me and assisting me. Without their help and encouragement it would not have been possible for me to undertake this work. I would like to thank all my friends for making my stay at NIT Rourkela lively and without their help this work would not have been possible.

(Ajit Kumar)

Date:

CONTENTS

LIST OF NOMENCLATURES

a	Crack length (mm)
a_0	Initial deflection of crack tip from bottom of notch
a_y	Projected crack length on Y-axis (mm)
a_x	Projected crack length on X-axis (mm)
A	Gauss Amplitude
A_0, A_1, A_2, A_3, A_4	Polynomial constants
B	Width of beam (mm)
c	Paris constant
C_0	Notch length (mm)
e	Eccentricity (mm)
E	Modulus of elasticity (MPa)
K	Stress intensity factor, SIF (MPa√m)
K_c	Critical stress intensity factor (MPa√m)
K_{Ic}	Critical Stress intensity factor for mode- I (MPa√m)
K_{max}	Maximum stress intensity factor (MPa√m)
K_{min}	Minimum stress intensity factor (MPa√m)
ΔK	Change in stress intensity factor range (MPa√m)
ΔK_{th}	Threshold of stress intensity range (MPa√m)
l	Span length (mm)
l_0	Minor span length (mm)
m	Exponent in the Paris equation
N	Number of cycle of fatigue life
N'	Delay cycle
N_c	Number of cycles at maximum deflection

R	Stress ratio
w	Gauss width (Gaussian width at half of maximum deflection)
W	Depth of beam (mm)
v	Poisson's ratio
Θ	Crack tip reference angle (Degree)
$\varnothing$	Hole Diameter (mm)
σ	Stress
σ_{uts}	Ultimate tensile strength
σ_{ys}	Yield stress
$f(g)$	Specimen geometrical factor of SIF
da/dN	Crack growth rate (mm/cycle)
da_y/dN	Projected crack growth rate (mm/cycle)

LIST OF FIGURES

LIST OF TABLES

ABSTRACT

Engineering components contain several defects. These defects are introduced during the extraction of the alloys and at various stages of manufacturing. Existence of defects such as, blow holes, slag inclusions, quench cracks, weld defects, notches, mechanical holes etc. are common in engineering materials and components. Their presence may reduce the load carrying capacity of the component and may cause immature failure in the both under monotonic and dynamic loading. These defects also interact with a propagating fatigue crack and may cause crack deflection, crack growth acceleration and even retardation. This investigation aims to study fatigue crack-hole interaction and prediction of crack path. The study has been made using 25×25 mm^2 cross section aluminium beam of span length 300 mm with circular hole of 3 mm diameter located at different positions. All fatigue tests were conducted using a 100 kN *BiSS* servo-hydraulic UTM. The tests were conducted under constant load amplitude condition maintaining a stress ratio, R=0.3. The monitoring of crack path was done by tip tracking method (TTM) using 10x magnification travelling microscope. The beams were subjected to constant amplitude load cycle under four-point bending loading condition. Presence of the hole deflected cracks from their normal paths. In some cases the cracks merged into the hole and resulted crack arrest. In the present work an attempt has been made to develop a model to predict the fatigue crack path.

Keywords: Fatigue crack-hole interaction, Fatigue crack propagation, Crack path prediction, Crack deflection.

CHAPTER 1

Introduction

1.1 Motivation and background of the present investigation

Beams find wide applications in engineering structures. During their service they are exposed to various monotonic as well as cyclic or fluctuating transverse load conditions. These may initiate new fatigue cracks from a highly stressed region or promote extension of existing cracks. These structures and components do contain blow holes, slag inclusions, quench cracks, weld defects, notches, mechanical holes etc. These discontinuities are introduced during extraction of metals and/or during various stages of fabrications. It is possible that stresses on the beams and other structural component may initiate new fatigue cracks from a highly stressed region and/or propagate existing flaws and cracks. The monitoring of crack during the course of their services is essential for stability of structure and safety. Several fracture mechanics based fatigue crack propagation models have been developed to predict fatigue crack behaviour and path. In mode-I loading condition the crack propagates in a straight path perpendicular to loading axis. The presence of defects such as, blow holes, slag inclusions, quench cracks, weld defects, micro crack, and mechanical hole has a major influence on the crack path and fatigue life of engineering component. Presence of a hole in the vicinity of crack path may cause the crack to deflect or merge into the hole [1, 2].

Estimation of fatigue crack growth rate and residual life prediction models are essential for safe operation and stability of structure. Fatigue crack-hole/notch interaction is available for CT and SENT specimen geometries [1, 2, 3].

In the present investigation an attempt has been made to study the influence of a mechanical hole in the vicinity of a propagating fatigue crack. In the present study the monitoring of deflected crack was by tip tracking method (TTM) using travelling microscope [4, 5].

1.2 Objectives of the work

The objectives of present investigation are:

- To study the effect of presence of a hole on fatigue crack propagation in a beam (SENB) under constant amplitude loading condition.
- To propose a model to predict fatigue crack path for a beam with a hole.

1.3 Thesis structure

The concept of present investigation is presented through six chapters. The chapter-1 presents an introduction of this investigation, 2nd chapter presents a brief review of literature. Chapter-3 describes the experimental procedure and methodology. Chapter-4 describes the results and discussion. Chapter-5 presents the formulation and validation of model for deflected crack path. Conclusions and possible future work are given in Chapter-6.

Plan of work is presented in the Fig. 1.1

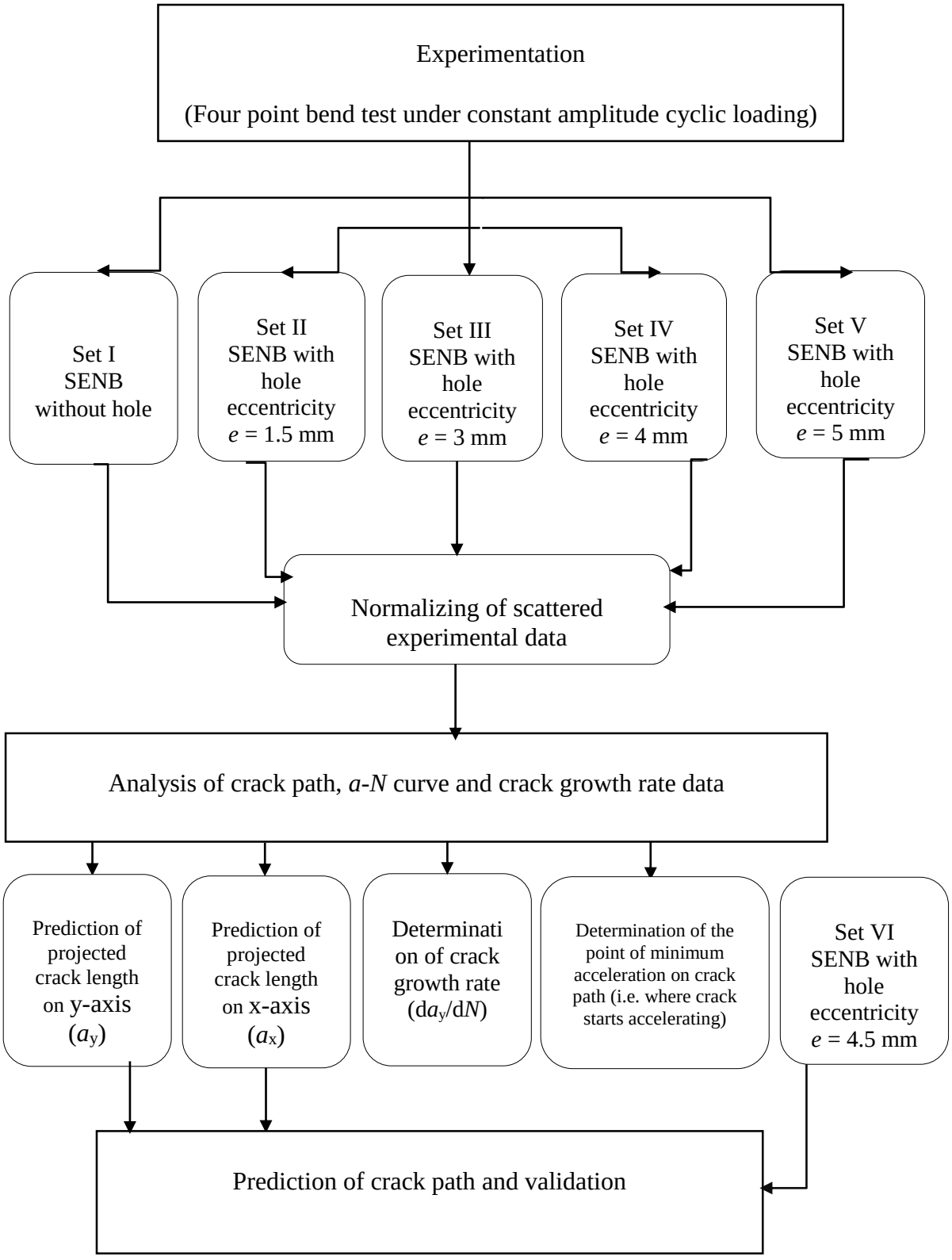

Fig. 1.1 Plan of work

CHAPTER 2

Literature review

2.1 Introduction

Fatigue in metals can be defined as failure of material due to the application of repeated or dynamic loads which are far less than that of static strength of material. In many cases the failure is insidious because it occurs without macroscopic warning. All engineering materials contain some defects. These defects are introduced in the material during their extraction and different stages of manufacturing and fabrication. A fatigue crack may originate from the surface or an interface (or from a dominating defect) during the course of service. A propagating crack may interact with defects and/or mechanical notch present in the material. This interaction may deflect, accelerate or even decelerate the propagating crack. The study is important as it can be used to predict deflected crack path and predict residual life of structure and component.

2.2 Regions of crack growth rate curve

A typical fatigue crack growth rate, da/dN vs. stress intensity factor (SIF) range, ΔK curve is illustrated in Fig. 2.1 [6]. The curve is divided into Regions- I, II and III on the basis of the slopes and nature of the curve.

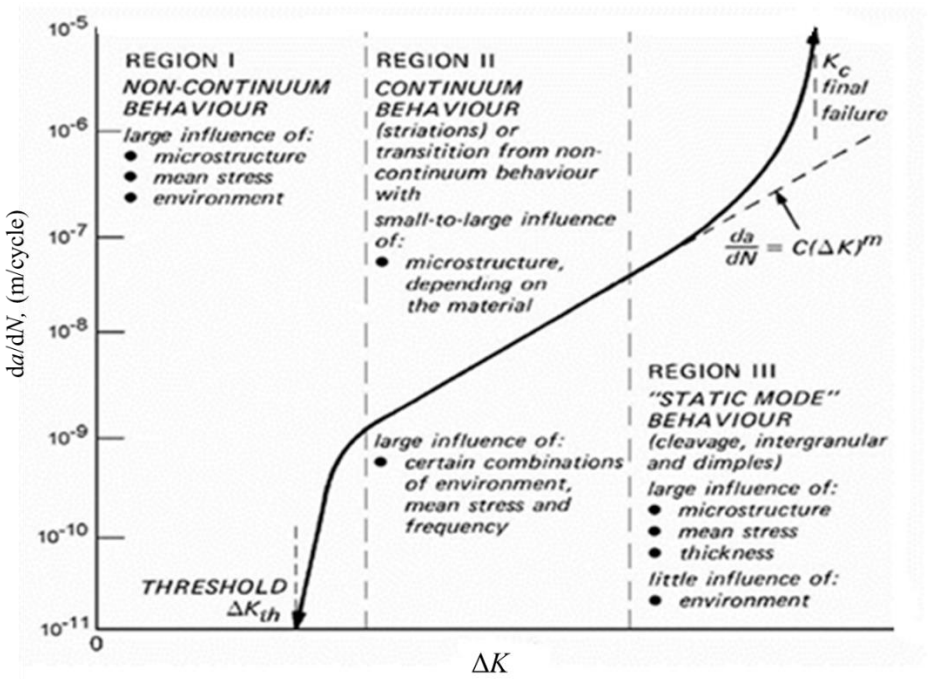

Fig. 2.1 Typical d*a*/d*N* versus log (Δ*K*) curve [6]

Region-I represents the early development of a fatigue crack and the crack growth rate. This region is microstructure sensitive and largely influenced by the microstructural features of the material (such as grain size, phases present and their morphology etc.), the mean stress of the applied load cycle, the operating temperature and the environment. The most important feature of this region is the existence of a critical stress intensity factor range below which fatigue cracks do not propagate. This value of SIF is termed as threshold of stress intensity range, ΔK_{th} [6].

Region- II represents the intermediate crack propagation range where the size of the plastic zone ahead of the crack tip is large compared to the mean grain size, but much smaller than the crack length [7]. The use of linear elastic fracture mechanics (LEFM) concepts is acceptable and the data follows a linear relationship between log (d*a*/d*N*) and log Δ*K*. This region corresponds to stable crack growth and the influence of microstructure, environment and thickness are small. The influence of the mean stress is probably the most significant [6].

Region- III

Region- III represents the fatigue crack growth at very high rates due to rapid and unstable crack growth just prior to final failure. The da/dN vs. ΔK curve becomes steep and asymptotically approaches the fracture toughness K_c/ K_{Ic} of the material. The corresponding stress level is very high and causes a large plastic zone near the crack tip. Since crack extension in this region is associated with large plastic zone, the influence of the nonlinear properties of the material cannot be ignored. The mean stress, materials microstructure and thickness have significant influence. On the other hand the environment has little influence. Fatigue crack propagation analysis is very complex in this region but is often ignored because it has little importance in most fatigue situations, the reason being high fatigue crack growth rate and little fatigue life is involved [6].

2.3 Interaction of propagating crack to defects and hole

Defects are introduced in the materials and machine/ structural components during various stages of metal extraction and fabrication. Presence of microscopic defects and macroscopic discontinuities may interact with a propagating crack. The stress fields associated with the crack and microstructural discontinuities and notch may deflect the crack from its usual path and may even cause crack acceleration or retardation depending upon the location of the notch and stress fields.

Tokaji *et al*. [8] studied the effect of microstructure defects on fatigue crack growth. They reported crack deflection and decrement of the crack growth rate at grain boundaries, triple points, phase interfaces. Ming Yuan *et al.* [9] observed that the crack impinging two dissimilar materials may get arrested or deflected at the interface. They compared energy release rate of deflected crack with the maximum energy release rate for a penetrating crack. The modulus

mismatch is reported to cause deflection of crack and development of a mixed-mode condition at the interface [10]. Microstructure and presence of second phase particles do affect the crack propagation behaviour [11, 12]. It is reported that the crack deflection around second phase particles results increase in toughness. The crack growth analysis are also done considering initial tilt and the maximum twist of the crack front between particles. This provided the basis for evaluating the deflection-induced reduction in crack driving force and toughening of the alloy. Toribio *et al.* [13] studied fatigue crack growth in pearlitic steel. It is reported that the main crack undergoes local deflection due to the presence of pearlite in the growth path of a crack and hence fracture toughening.

Mechanical notches and stress distribution around notch also influence the crack path and growth rate. It is reported that the introduction of compressive stress field by expanding a hole at the crack tip resulted arrest of growing crack [14,15]. Introducing compressive stress field just by inserting pins into holes, drilled in the vicinity of the crack tips, is an effective method for retarding crack growth [16]. Anggit Murdani *et al.* [17] analysed stresses at the periphery of holes using a software for two-dimensional elastic problems. The information may be used to predict path and growth rate of a fatigue crack.

2.4 Prediction Fatigue crack direction

Fatigue crack data are important parameters for structural design. Most of the research works predict the crack direction by FEM simulation. However, only the direction of crack extension is predicted which is of limited applicability [18].

The most common approach to evaluate the fatigue life is based on experimental data relating stress/ strain and number of cycles to failure of smooth specimens. Most often the design stress data are incorporated with a factor of safety. With the development of fracture mechanics and

competitive design requirement, many researchers are now applying the damage tolerance methodology. As per this approach, the details of defects in terms of their size, distribution, position etc. should be known. Fatigue crack path or direction of crack extension are important for structural design.

Maximum tangential stress criterion **(MTS criterion):** This is one of the widely used theories of failure. Erdogan and Sih [19] used this theory to study growth of deflected. The criterion states that: (i) crack propagation starts from tip of a crack along the radial direction, on which the tangential stress becomes maximum and (ii) fracture starts when the maximum tangential stress reaches a critical stress equal to fracture stress in uniaxial tension.

Minimum strain energy density criterion **(S-criterion):** This criterion was used by Sih [20, 21] and is based on the local density of the energy field in the crack tip region. The crack is assumed to grow in a direction along which the strain energy density factor reaches a minimum value and fracture occurs when this value reaches a critical value.

The J-criterion**:** This criterion was used by Sih, G. C. [22] in an attempt to apply path independent line integrals to study the problem of crack growth under mixed mode loadings. This criterion states that: (i) a crack extends along the direction of vector *J* and (ii) fracture occurs when this vector *J* reaches a critical value.

Dilatational strain energy density criterion **(T-criterion):** Theocaris and Andrianopoulos [23] and Theocaris *et al*. [24] proposed this criterion. Strain energy density is the basis of this criterion also. However, the investigators suggested separation of the total strain energy density into its distortional and dilatational components. This criterion states that (i) a crack starts to propagate when the dilatational strain energy at a point in the vicinity of its tip reaches a critical

value, and (ii) the elastic-plastic boundary obtained from the Mises yield condition is used to evaluate the dilatational strain energy around the crack tip.

In most of the available literature crack path prediction and life estimation have been done with defect located in the path of the crack. However the defects located off from the crack path do affect the crack propagation behaviour. The stress field around the defects and ahead of the crack tip dictate the crack path and may result crack growth acceleration or deceleration. It is also worth to mention that large crack path alteration may also affect structural integrity. Present investigation aims to investigate the effect of an off located notch on fatigue crack path.

CHAPTER 3

Experimental investigation

3.1 Introduction

This chapter deals with details of material, specimen geometry and loading set-up for conducting fatigue crack growth studies. The main objective of this investigation is to study the fatigue crack deflection and its propagation in the presence of a hole. The details of the crack monitoring methodology is also described.

3.2 Material and specimen

The material used in the present investigation is a commercial 1050A aluminium in the form of 25 mm square beam. The tensile test specimens were fabricated following ASTM E8 [25] standard. The dimensional details of tensile specimen and tensile properties are presented in in Table 3.1.

Table 3.1 Dimensional details of tensile specimen and tensile properties

Gauge length	30 mm	Yield strength, σ_{ys}	170 MPa
Gauge diameter	6.11 mm	Ultimate tensile strength, σ_{uts}	249 MPa
Grip distance	100 mm	Modulus of elasticity (E)	69 GPa
Grip diameter	10.82 mm	Poisson's ratio (ν)	0.33

The single edge notched beam specimens were fabricated from the supplied 25 mm square beams. Straight vertical notch of length 3 mm was machined by wire EDM in a beam of span length 300 mm containing a hole of diameter 3 mm at a distance 7.5 mm from the top face of the beam (i.e., y-coordinate 7.5 mm). The objective of present investigation is to study the effect of hole position on crack path. Circular holes were made at various eccentricities (x-

coordinates): 1.5, 3, 4, 4.5, and 5 mm from notch centre line. Dimensional details of the specimens used in this investigation are given in Table 3.2. All fatigue crack growth tests were conducted in 4-point bending mode. The detailed dimensions of the specimen, notch, diameter of hole, hole locations and loading configurations are presented in Fig. 3.1. Photograph of a typical test specimen is illustrated in Fig. 3.2.

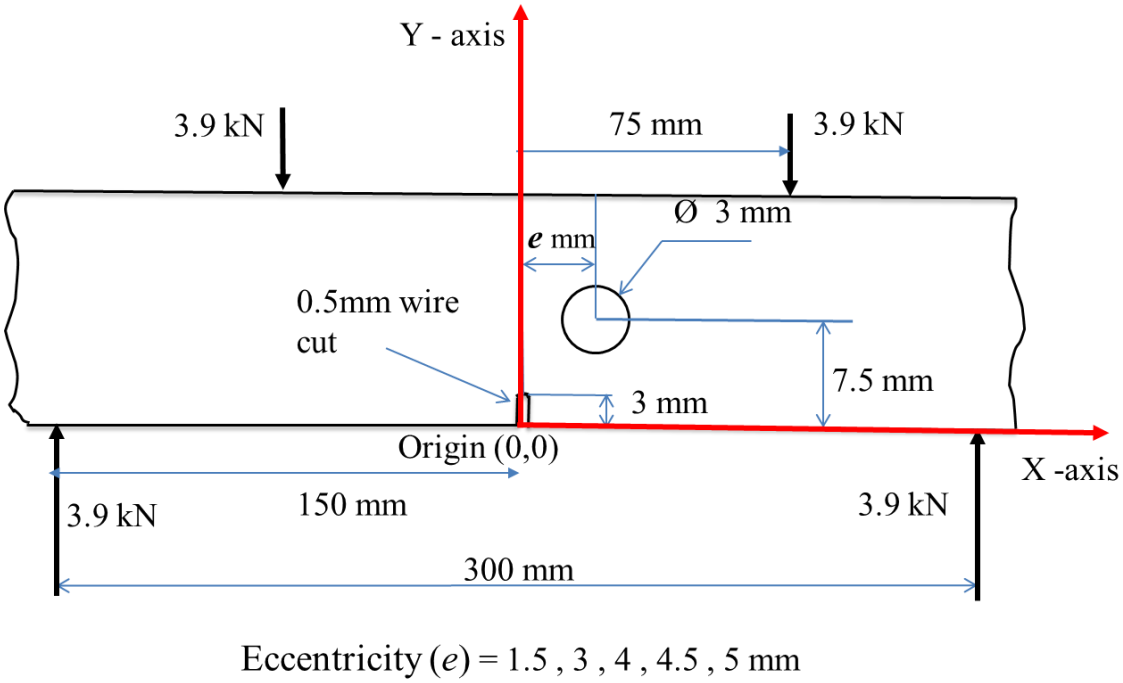

Fig. 3.1 Dimensional details of the beam specimen (with hole and notch) and loading configuration

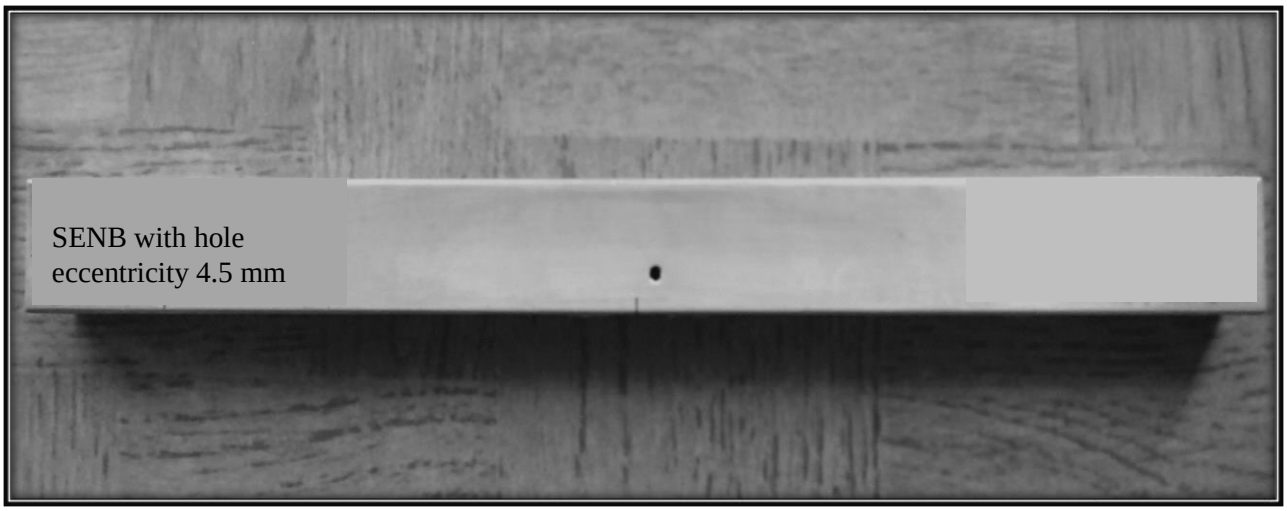

Fig. 3.2 Photograph of the test specimen

Table 3.2 Dimensional details of the 25 mm square beam specimens

Specimen parameters	**Dimension (mm)**
Span length (*l*)	300
Minor span length (l_0)	150
Width (*B*)	25
Depth (*W*)	25
Notch length (C_0)	3
Hole diameter (*Ø*)	3
Eccentricities (*e*)	1.5, 3, 4, 4.5, 5

3.3 Test specimen and accessories

All fatigue crack growth tests were conducted in 4-point bending mode using a100 kN *BiSS* servo-hydraulic universal testing machine interfaced to a computer for machine control and data acquisition. Both sides of the specimen surfaces were polished to facilitate easy monitoring

of the crack. The presence of hole is expected to deflect the crack during its growth. Therefore, the monitoring of crack path was done by tip tracking method (TTM) using 10x travelling microscope. Fig. 3.3 shows an overall arrangement of the test set-up along with the test specimen. . **F**atigue cracks emanating from notch can be seen in the macrogrphs in Fig. 3.4

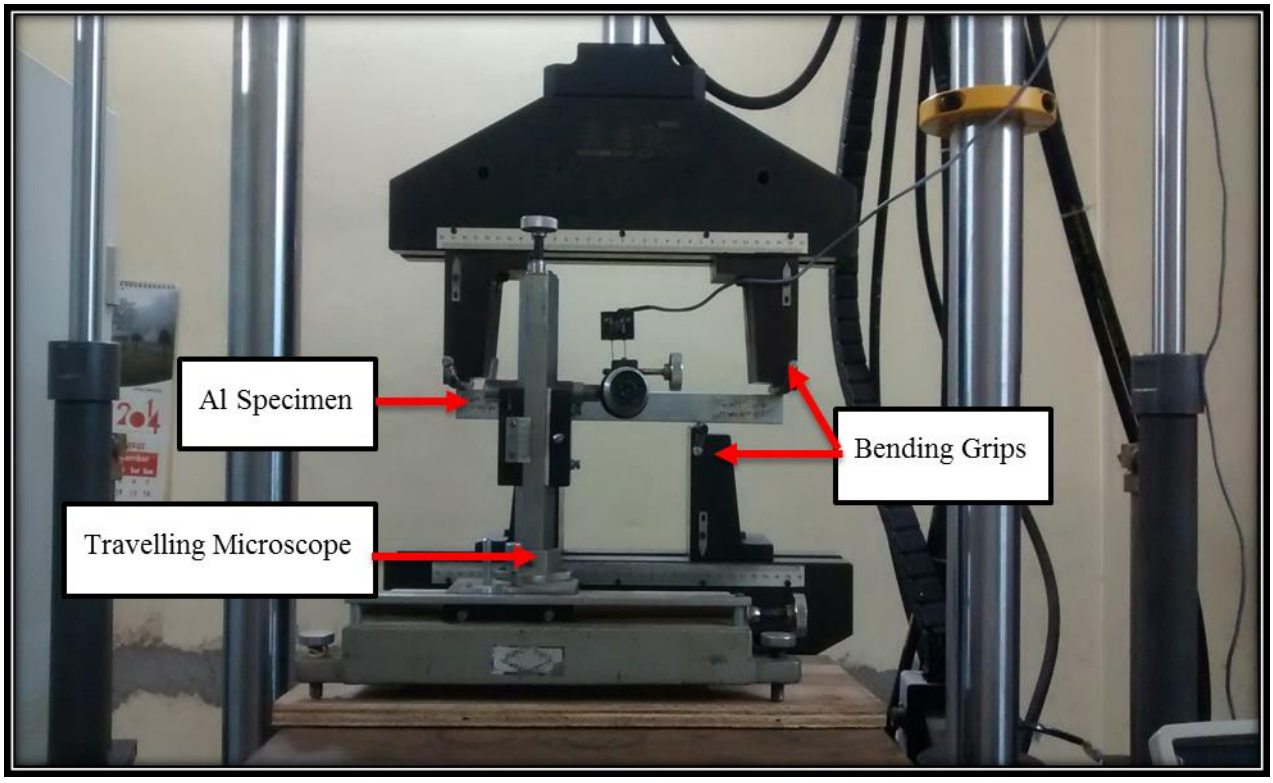

Fig.3.3 Four point bend set-up and travelling microscope for crack monitoring

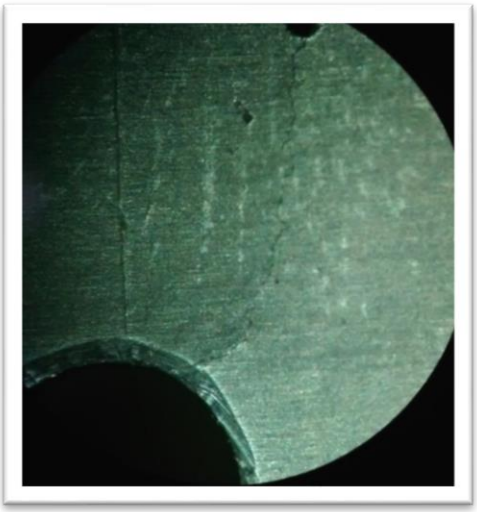

Fig. 3.4 (a)

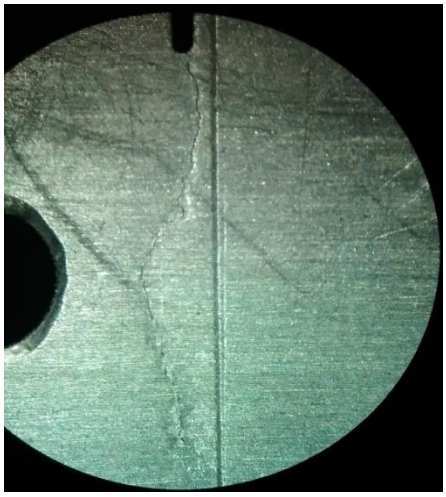

Fig. 3.4 (b)

Fig. 3.4 Macroscopic view of two specimens. Fatigue cracks emanating from notch can be seen in the macrogrphs for eccentricity, (a) e = 1.5 mm, the crack merges into the hole, (b) e = 4 mm, the crack deflects.

3.4 Test condition

All tests were conducted at room temperature and normal environment condition. Following is the loading details of the specimen during test:

Constant sinusoidal load amplitude, operated under load control mode

Stress ratio, R=0.3

Maximum load, P_{max} = 7.8 kN

Frequency = 3 Hz

3.5 Crack monitoring

The present investigation deals with fatigue crack-circular hole interaction. In the absence of a hole, crack propagation occurs in a direction transverse to the span length. However, presence of a hole deflects the crack from its normal path. Since a deflected crack cannot be monitored using a COD gauge, the same was done by tip tracking method (TTM) using a 10x travelling microscope [4, 5].

CHAPTER 4

Results and discussion

4.1 Introduction

This chapter deals with experimentally generated crack growth data and their analysis. As expected, the presence of circular hole has deflected the crack from the usual path transverse to the span length. Attempt has been made to correlate the deflection of the crack with the position of the hole and study the effect of the stress field in the proximity of crack tip and hole. An attempt has also been made to predict crack path when emanating or propagating crack path interacts with mechanical hole.

4.2 Results and Discussion

The crack path in the aluminium beam with and without circular hole have been shown in Fig. 4.1. In the absence of hole, crack propagated transverse to the span length. On the other hand the presence of hole caused deflection of crack from its usual expected path. The merger of the crack took place in case of the holes centred at coordinates (1.5, 7.5) and (3.0, 7.5). The holes centred at coordinates (4.0, 7.5) and (5.0, 7.5) have only deflected the cracks from the path and maximum is noticed for hole cantered at (4.0, 7.5). The projection of deflected crack on y-axis is termed as a_y and the same on x-axis as a_x [1]. The deflection of crack path due to the presence of hole during the constant amplitude cyclic loading is illustrated in Fig. 4.2 in the form of projected crack length (a_y) vs. number of load cycles (N).

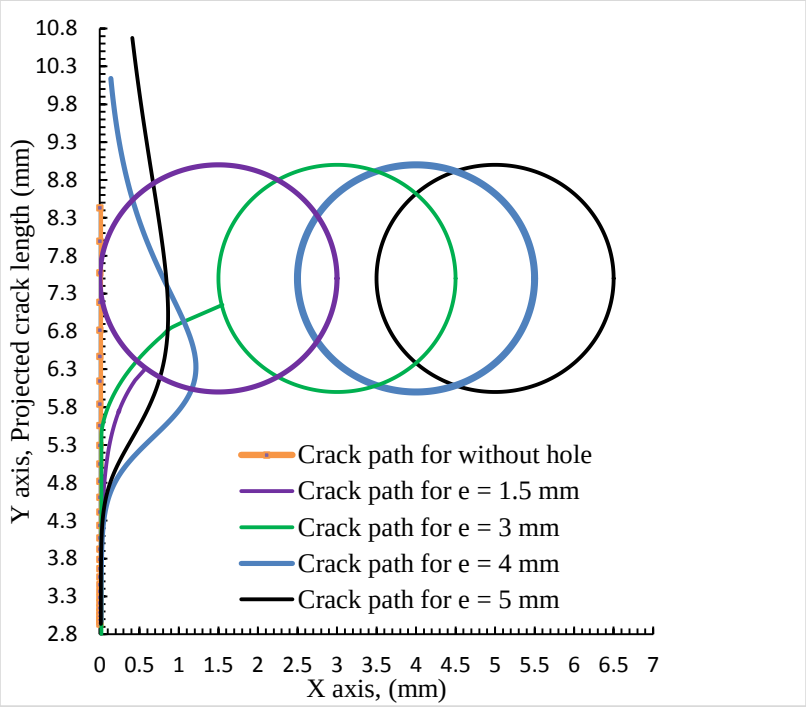

Fig. 4.1 Superimposed plot of crack path with hole for different eccentricity

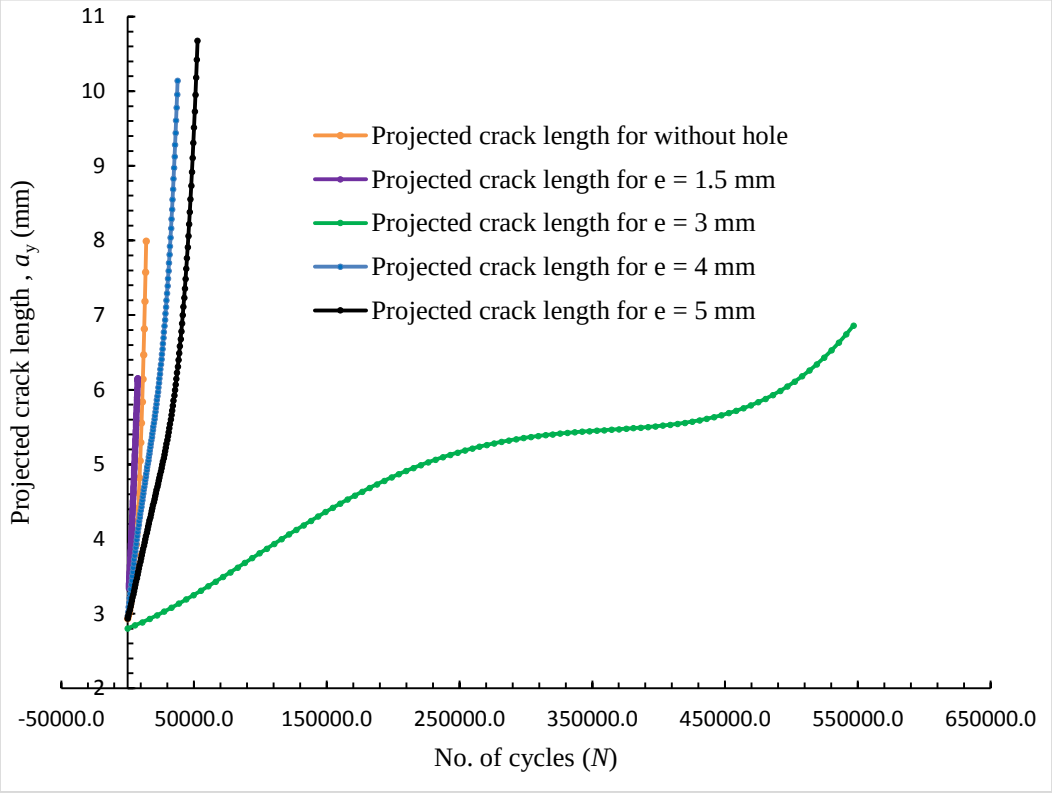

Fig. 4.2 Plot of a_y vs. N for different eccentricities

The presence of a hole in the beam has resulted in a crack growth acceleration or deceleration depending on the eccentricity of the hole. The hole centered at (1.5, 7.5) caused marginal increase in crack growth rate. On the other hand, deceleration in the crack growth rate is noticed for other hole positions and maximum crack growth retardation occurred for hole centered at (3.0, 7.5).

The compressive stresses are known to retard or decelerate a growing fatigue crack. In the Figs. 4.3 and 4.4, stress field around the crack path have been presented for hole eccentricities 4 mm and 3 mm respectively, using *FRANC 2D* software. Both the figures show the presence of compressive stress field in the wake of crack path. It can be observed that for e = 4 mm the wake is surrounded in a uniform compressive stress field. However, the crack path for the hole at e = 3 mm is enclosed in a compressive stress field of much higher magnitude. Due to the presence of compressive stress field that is much higher in magnitude the crack growth rate in case of e = 3 mm is lower.

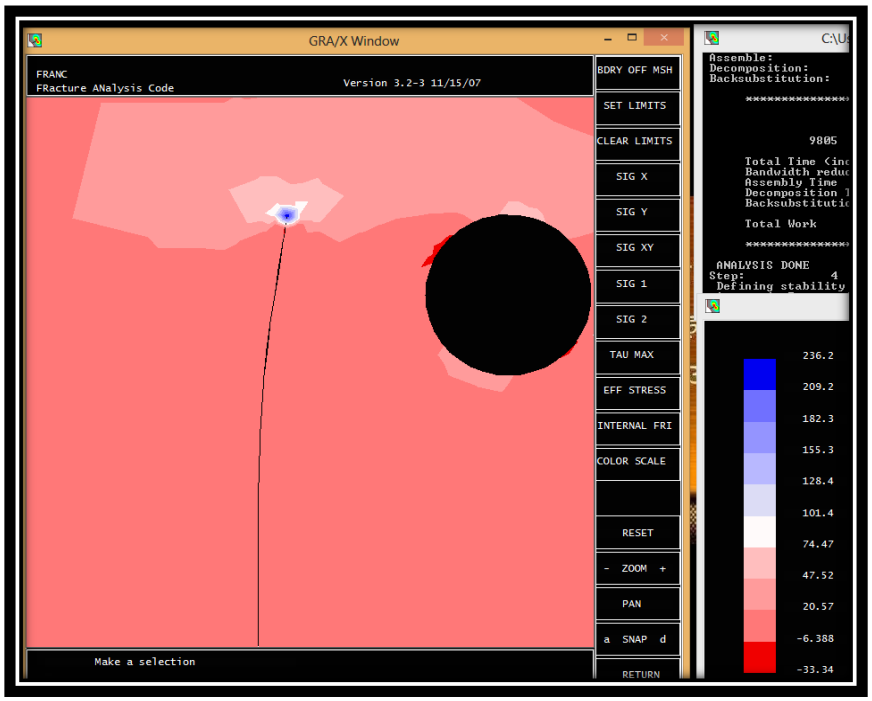

Fig.4.3 Stress pattern around crack path e, 4 mm (stress in ksi)

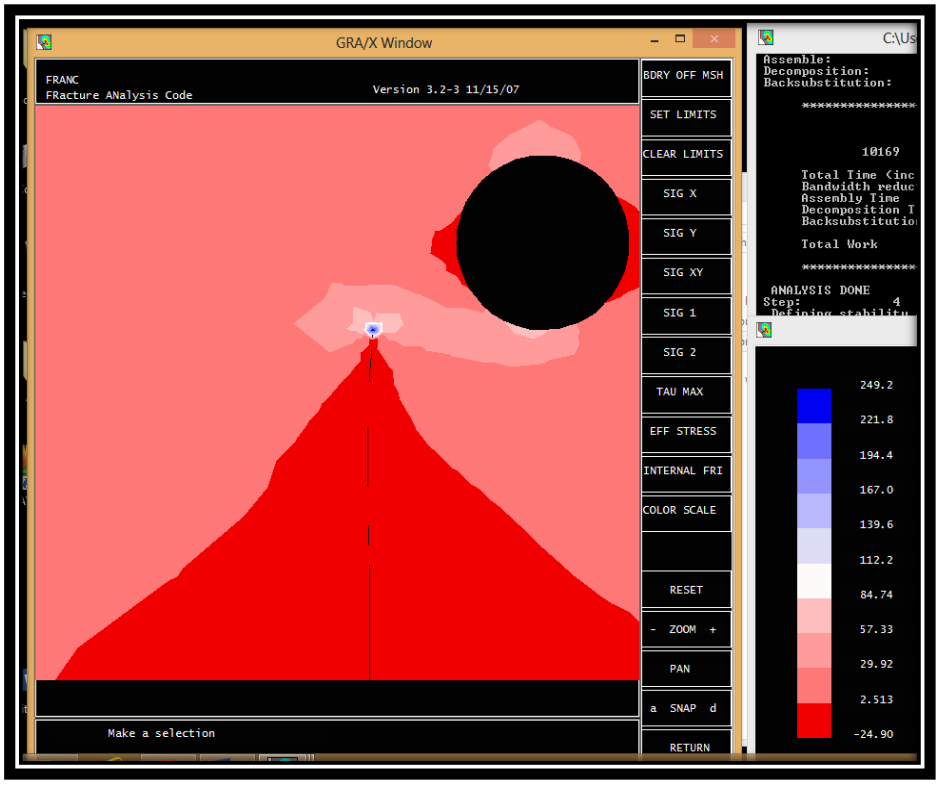

Fig.4.4 Stress pattern around crack path *e*, 3 mm (stress in ksi)

It can be seen from Fig. 4.2 that, for beams with e = 3 mm, crack starts to accelerate at a_y = 6.1 mm, and this point has been taken as reference. We now define a term delay cycle (N') which refers to the additional number of cycles required to reach a projected crack length a_y = 6.1 mm compared to a beam having no hole.

Fig. 4.5 shows a plot of delay cycle (N') for various eccentricities. It can be seen in this figure that eccentricity of the hole has resulted in marginal positive or negative delay cycles however the hole located at eccentricity 3 mm resulted in N' close to 6 x10^6 cycles.

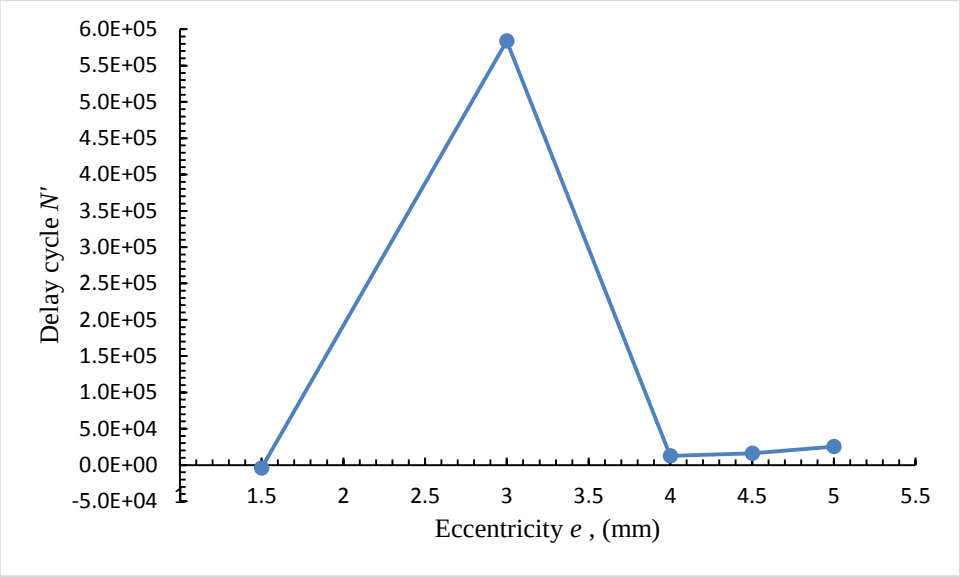

Fig. 4.5 Plot of *N'* vs. Eccentricity *e*, (mm)

The deflection of crack due to the presence of hole is shown in Fig 4.2. The effects of eccentricity of hole on crack deflection is illustrated in Fig. 4.6. The maximum crack tip deflection took place in beams having eccentricity 3 mm. As eccentricity is increased the crack path becomes flattened (Fig. 4.1) and the maximum deflection decreases.

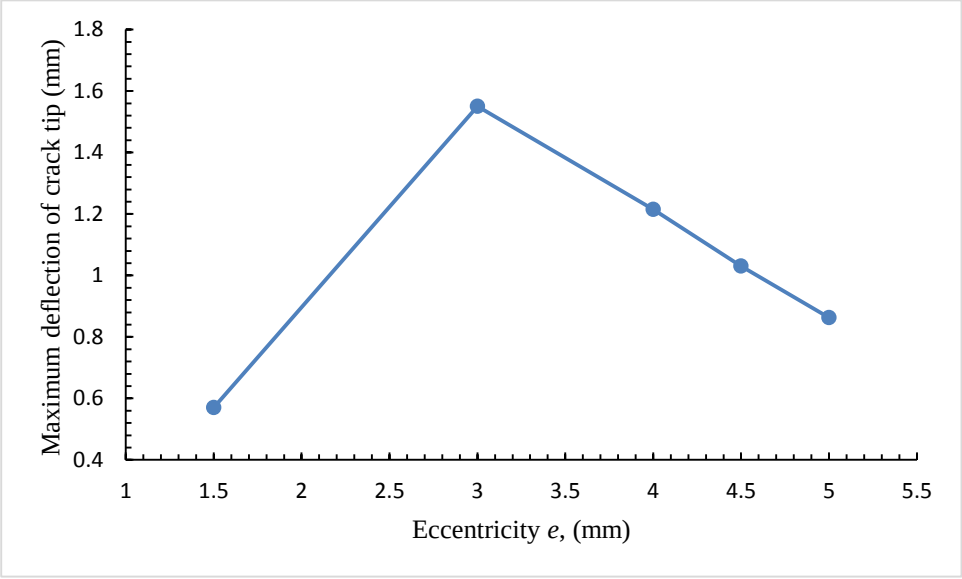

Fig. 4.6 Plot of Maximum deflection crack tip vs Eccentricity

The deflection of a crack path depends not only on eccentricity but also on the position of crack tip with respect to the centre of the hole. This is expressed by a new parameter, *crack tip reference angle* (Θ), defined by the angle subtended by the line joining the instantaneous crack tip position and the centre of the hole and illustrated in Fig.4.7.

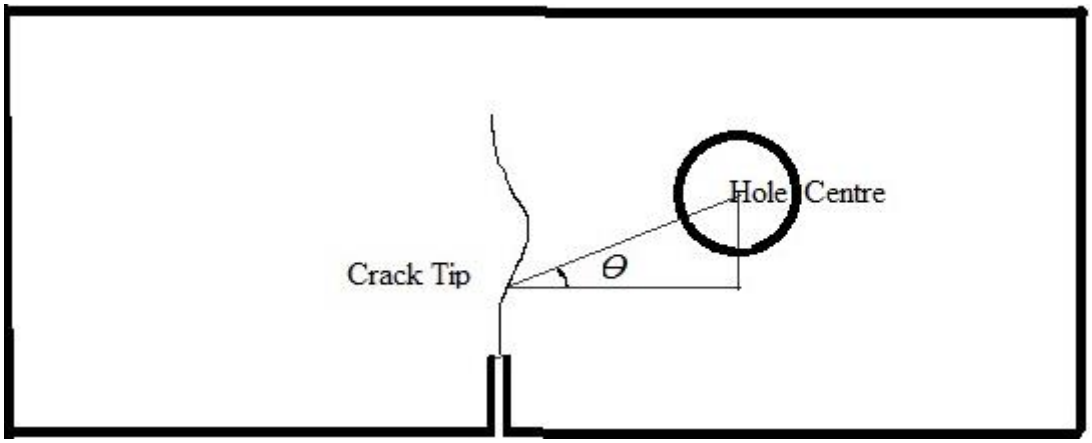

Fig. 4.7 Definition of angle (Θ)

The presence of hole has resulted in crack path deflection, and merger when the hole is situated close to the emanating crack path and the same is illustrated in Fig. 4.1. The deflection of crack path due to the presence of hole during the constant amplitude cyclic loading is illustrated in Fig. 4.8 in the form of projected crack length (a_y) vs. Θ. From Fig.4.8. it is observed that crack path having eccentricity 1.5 mm and 3 mm merge to the hole below centre (a_y = 7.5 mm).

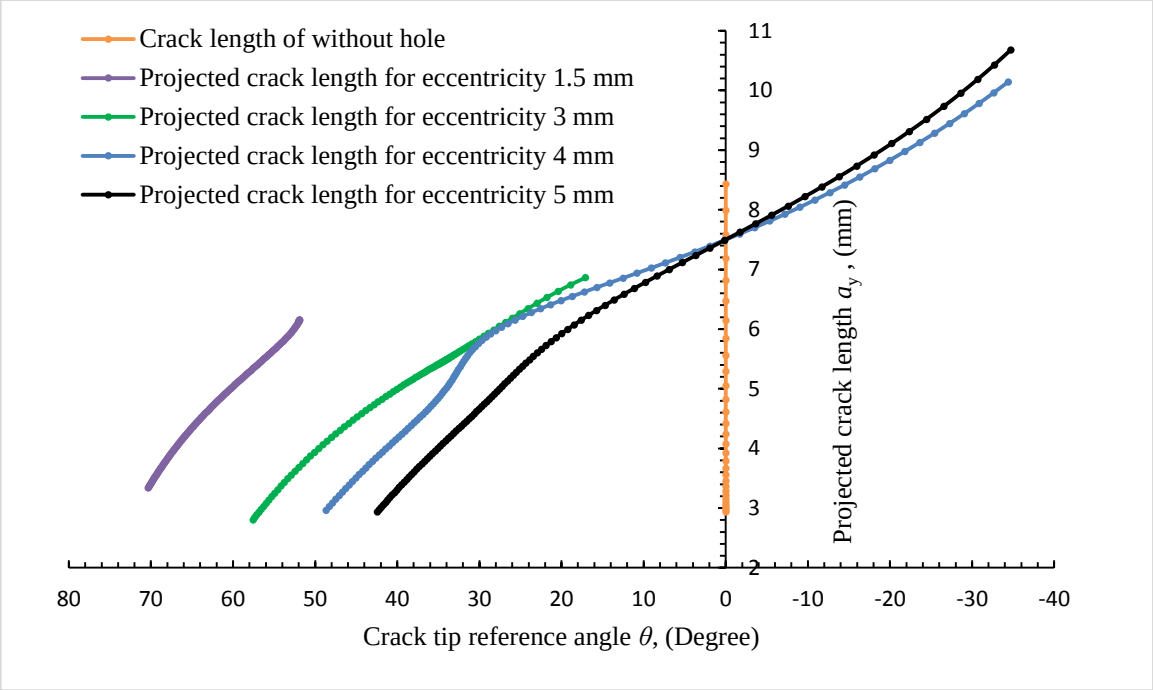

Fig. 4.8 Plot of projected crack length (a_y) vs. crack tip reference angle (Θ)

The effect of hole on crack growth rate is illustrated in Fig.4.9. It can be observed that for e = 1.5 mm, the crack growth rate steadily increases till the crack merges into the hole. For e = 3 mm, the crack growth rate is very small because of the presence of compressive stress field as explained earlier. FCGR slightly increases when the crack approaches the hole just before merger. For e = 4 mm and 5 mm, there is an initial decrease in crack growth rate after which it starts increasing.

The values of θ where the minimum crack growth rate takes place are different for each value of eccentricity. Therefore, a plot (Fig. 4.10) is made showing the variation of $\theta_{minimum}$ with non-dimensional eccentricity given by $ø/e$ where $ø$ is the diameter of the hole. For a particular value of eccentricity ratio ($ø/e$), the value of θ at which minimum crack growth occurs can be known from the graph and that is the point beyond which crack growth accelerates. Thus, once the crack path is predicted, it is possible to identify the point on the crack path where minimum

crack growth rate occurs (Fig. 5.1). Crack path prediction has been made in Chapter-5 and the point on the crack path beyond which the crack growth accelerates has been marked.

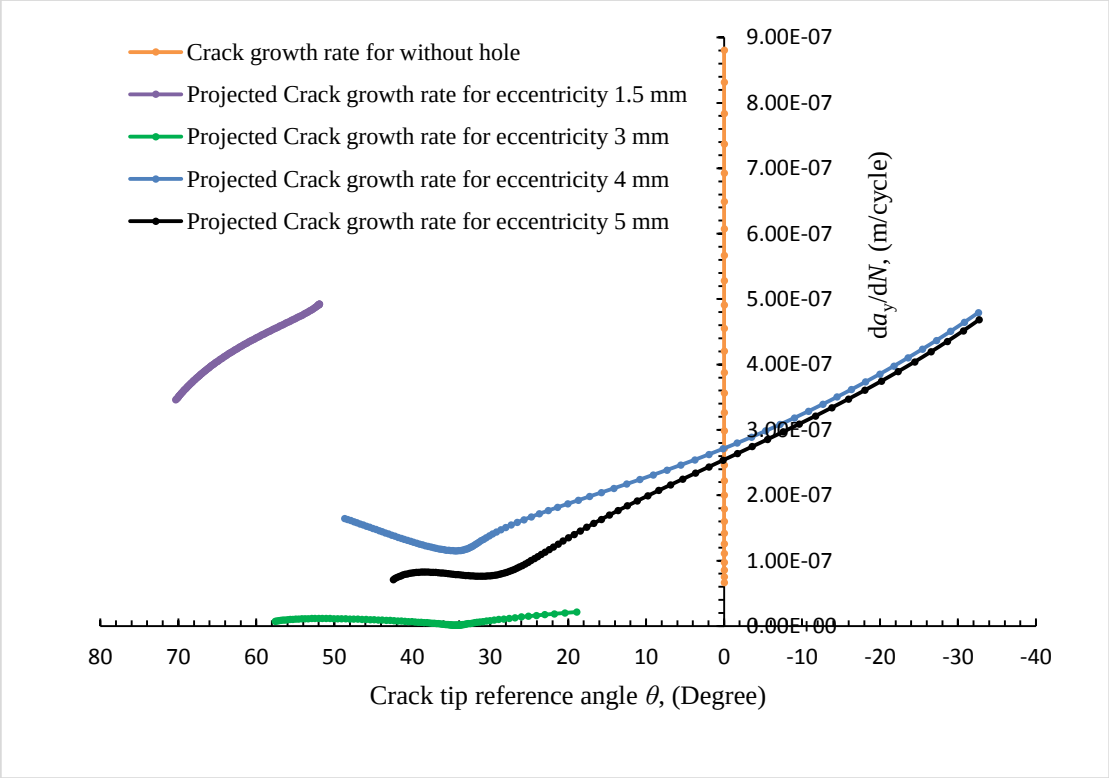

Fig. 4.9 Projected crack growth rate (da_y/dN) vs. Crack tip reference angle θ, (Degree)

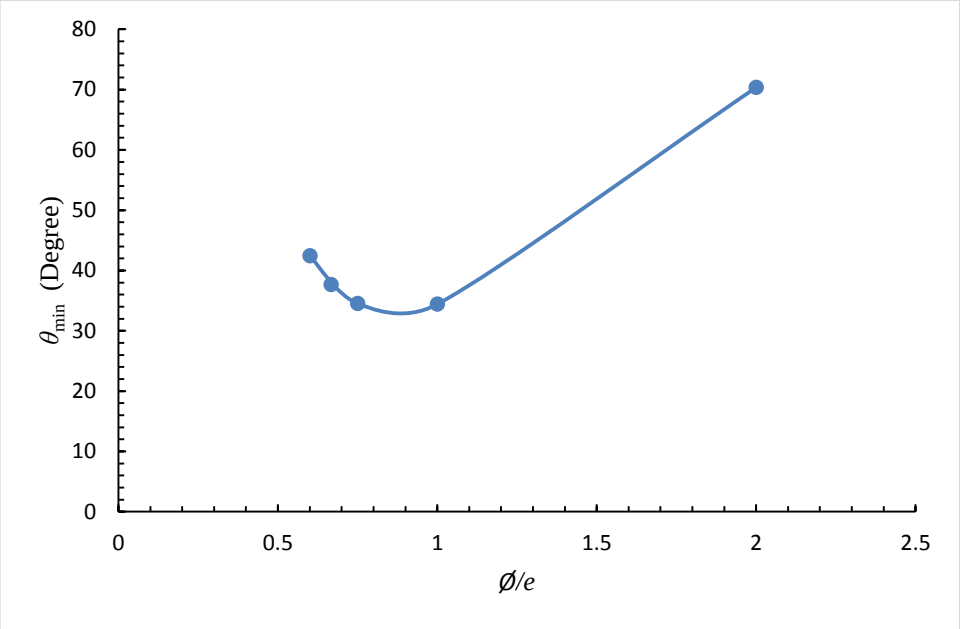

Fig. 4.10 Plot of Θ_{min} vs. $\emptyset/e$

The variation of range of stress intensity factor (SIF) with angle (Θ) is illustrated in Fig. 4.11. The stress-intensity factor for a beam in bending that contains an edge crack is calculated by equation (4.1) [25]

$$K_I = \frac{6M}{B.(W - a_y)^{3/2}} . f\left(\frac{a_y}{W}\right) \tag{4.1}$$

where M is the moment, $f\left(\frac{a_y}{W}\right)$ is geometrical factor , a_y projected crack length, B beam thickness and W is width of beam

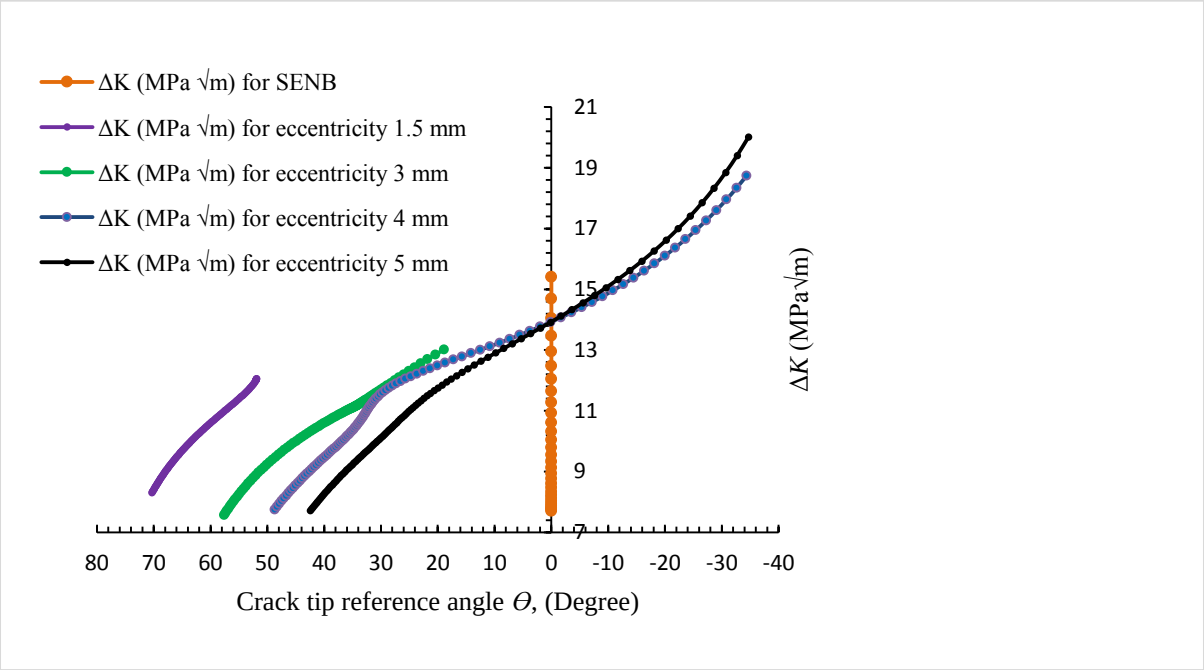

Fig. 4.11 ΔK vs. crack tip reference angle (Θ)

CHAPTER 5

Prediction of Fatigue crack path

5.1 Introduction

This chapter explains an approach for predicting fatigue crack path. A fatigue crack path in mode-I propagates in the plane of the notch in the absence of any hole, or when there is no hole-crack interaction. The presence of a hole near the propagating crack interacts with the crack path and the crack deflects or sometimes merges into the hole. It is, therefore, necessary to predict the crack path.

In the present investigation an attempt has been made to predict crack path in a beam when emanating or propagating crack path interacts with a mechanical hole. Here crack path is predicated in two separate steps: (i) Projection of deflected crack path on x-axis termed as a_x, (ii) Projection of deflected crack path on y-axis termed as a_y. The reference axes are shown in Fig. 3.1.

5.2 Procedure to predict crack path

The constant amplitude fatigue crack growth tests were conducted on six sets of (SENB) specimens: (i) without hole (ii) eccentricity 1.5 mm (iii) eccentricity 3 mm (iv) eccentricity 4 mm (v) eccentricity 4.5 mm (vi) eccentricity 5 (three for each category). Prediction of a_x and a_y are done separately. The prediction of a_x has been done using Gauss amplitude model and prediction of a_y has been done using polynomial curve fitting.

Method of predicting a_x:

Gauss amplitude model is used for predicting a_x.

The form of Gauss amplitude function for proposed model is as follow:

$$a_x = a_0 + Ae^{-\frac{(N-N_C)^2}{2w^2}} \quad (5.1)$$

a_x -Deflection of crack tip at N number of cycle (mm)

a_0 -Initial deflection of crack tip from bottom of notch or, from Y axes (mm)

A- Gauss amplitude

N - Number of cycle

N_c- Number of cycles at maximum deflection

w – Gauss width (Gaussian function at half of maximum deflection)

All the constants have been evaluated for eccentricities 1.5, 3, 4, 5 mm (Table 5.1).

Table 5.1 Experimental Gauss Amplitude constants Table For a_x

Coordinate of hole centre	a_0 (Offset) mm	N_c (Horizontal mid-point)	w (Gauss width)	A (Peak Amplitude)
1.5,7.5	0.0124	62482.5	8534.00	410358000
3,7.5	0.01923	1.34085E6	154130.19	28407.92
4,7.5	0.01492	25026.94267	5921.18	1.20
5,7.5	0.01277	41585.83931	9017.07	0.85

Table 5.2 Interpolated Gauss Amplitude constants Table For a_x

Eccentricity (mm)	***Interpolated*** a_0 , ***mm***	***Interpolated*** N_c	***Interpolated w***	***Interpolated A***
1.5	0.0124	62482.5	8534.005	4.10E+08
1.57143	0.01273	123316.6667	15467.15694	3.91E+08
1.64286	0.01305	184150.8333	22400.30889	3.71E+08
1.71429	0.01338	244985	29333.46083	3.52E+08
1.78571	0.0137	305819.1667	36266.61277	3.32E+08
1.85714	0.01403	366653.3333	43199.76471	3.13E+08
1.92857	0.01435	427487.5	50132.91666	2.93E+08
2	0.01468	488321.6667	57066.0686	2.74E+08
2.07143	0.015	549155.8333	63999.22054	2.54E+08
2.14286	0.01533	609990	70932.37249	2.35E+08
2.21429	0.01565	670824.1667	77865.52443	2.15E+08
2.28571	0.01598	731658.3333	84798.67637	1.95E+08
2.35714	0.0163	792492.5	91731.82831	1.76E+08
2.42857	0.01663	853326.6667	98664.98026	1.56E+08
2.5	0.01695	914160.8333	105598.1322	1.37E+08
2.57143	0.01728	974995	112531.2841	1.17E+08
2.64286	0.0176	1.04E+06	119464.4361	9.77E+07
2.71429	0.01793	1.10E+06	126397.588	7.82E+07
2.78571	0.01825	1.16E+06	133330.74	5.86E+07
2.85714	0.01858	1.22E+06	140263.8919	3.91E+07
2.92857	0.0189	1.28E+06	147197.0439	1.96E+07
3	0.01923	1.34E+06	154130.1958	28407.92363
3.07143	0.01892	1.25E+06	143543.8378	26378.87196
3.14286	0.01861	1.15E+06	132957.4797	24349.82028
3.21429	0.01831	1.06E+06	122371.1217	22320.76861
3.28571	0.018	964293.4122	111784.7636	20291.71694
3.35714	0.01769	870366.7652	101198.4056	18262.66526
3.42857	0.01738	776440.1183	90612.04753	16233.61359
3.5	0.01707	682513.4713	80025.68948	14204.56191
3.57143	0.01677	588586.8244	69439.33143	12175.51024
3.64286	0.01646	494660.1774	58852.97339	10146.45857
3.71429	0.01615	400733.5305	48266.61534	8117.40689
3.78571	0.01584	306806.8835	37680.2573	6088.35522
3.85714	0.01554	212880.2366	27093.89925	4059.30355
3.92857	0.01523	118953.5896	16507.54121	2030.25187
4	0.01492	25026.94267	5921.18316	1.2002
4.07143	0.0116	26118.77512	6171.42649	1.17715
4.14286	0.00827	27210.60758	6421.66983	1.15411
4.21429	0.00495	28302.44003	6671.91316	1.13106
4.28571	0.00163	29394.27249	6922.15649	1.10801
4.35714	-0.00169	30486.10494	7172.39982	1.08496
4.42857	-0.00502	31577.9374	7422.64316	1.06192
4.5	-0.00834	32669.76985	7672.88649	1.03887
4.57143	-0.00532	33943.49406	7864.91311	1.01193
4.64286	-0.00231	35217.21827	8056.93974	0.985
4.71429	7.07E-04	36490.94248	8248.96636	0.95806
4.78571	0.00372	37764.66668	8440.99298	0.93113
4.85714	0.00674	39038.39089	8633.0196	0.90419
4.92857	0.00975	40312.1151	8825.04623	0.87726
5	0.01277	41585.83931	9017.07285	0.85032

Method of predicting a_y:

Fatigue crack path (a_y) is predicted using polynomial curve fitting. The form of polynomial equation for proposed model is as follow:

$$a_y = A_0 + A_1N^1 + A_2N^2 + A_3N^3 + A_4N^4 \quad (5.2)$$

a_y is propagating crack length on y-axis (mm)

N is number of cycles

A_0, A_1, A_2, A_3, A_4 all are polynomial constants.

All the constants have been evaluated for eccentricities 1.5, 3, 4, 5 mm (Table 5.2).

Table 5.3 Experimental Polynomial Constants Data Table For a_y

	A_0	**A_1**	**A_2**	**A_3**	**A_4**
Centre (1.5,7.5)	3.03974291	3.25765909E-04	1.09402855E-08	0	0
Centre (3,7.5)	2.76042361	- 1.09326214E-05	1.53777738E-10	- 4.16269090E-16	3.41816951E-22
Centre (4,7.5)	2.96422	1.65295E-04	-2.02594E-09	-4.76122E-14	3.16777E-18
Centre (5,7.5)	2.93685026	7.01422370E-05	1.78436875E-09	- 1.03654004E-13	1.84838608E-18

Table 5.4 Interpolated polynomial constants Table For a_y

Eccentricity e (mm)	***Interpolated A_0***	***Interpolated A_1***	***Interpolated A_2***	***Interpolated A_3***	***Interpolated A_4***
1.5	3.04	3.26E-04	1.09E-08	0.00E+00	0
1.57143	3.02669	3.10E-04	1.04E-08	-1.98E-17	1.63E-23
1.64286	3.01337	2.94E-04	9.88E-09	-3.96E-17	3.26E-23
1.71429	3.00006	2.78E-04	9.36E-09	-5.94E-17	4.89E-23
1.78571	2.98675	2.62E-04	8.85E-09	-7.92E-17	6.51E-23
1.85714	2.97343	2.46E-04	8.34E-09	-9.90E-17	8.14E-23
1.92857	2.96012	2.30E-04	7.83E-09	-1.19E-16	9.77E-23
2	2.94681	2.14E-04	7.32E-09	-1.39E-16	1.14E-22
2.07143	2.93349	1.98E-04	6.81E-09	-1.58E-16	1.30E-22
2.14286	2.92018	1.82E-04	6.29E-09	-1.78E-16	1.47E-22
2.21429	2.90687	1.66E-04	5.78E-09	-1.98E-16	1.63E-22
2.28571	2.89356	1.50E-04	5.27E-09	-2.18E-16	1.79E-22
2.35714	2.88024	1.33E-04	4.76E-09	-2.38E-16	1.95E-22
2.42857	2.86693	1.17E-04	4.25E-09	-2.58E-16	2.12E-22
2.5	2.85362	1.01E-04	3.74E-09	-2.77E-16	2.28E-22
2.57143	2.8403	8.54E-05	3.22E-09	-2.97E-16	2.44E-22
2.64286	2.82699	6.93E-05	2.71E-09	-3.17E-16	2.61E-22
2.71429	2.81368	5.33E-05	2.20E-09	-3.37E-16	2.77E-22
2.78571	2.80036	3.72E-05	1.69E-09	-3.57E-16	2.93E-22
2.85714	2.78705	2.12E-05	1.18E-09	-3.76E-16	3.09E-22
2.92857	2.77374	5.14E-06	6.66E-10	-3.96E-16	3.26E-22
3	2.76042	-1.09E-05	1.54E-10	-4.16E-16	3.42E-22
3.07143	2.77498	1.66E-06	-1.71E-12	-3.79E-15	2.27E-19
3.14286	2.78954	1.42E-05	-1.57E-10	-7.16E-15	4.53E-19
3.21429	2.80409	2.68E-05	-3.13E-10	-1.05E-14	6.80E-19
3.28571	2.81865	3.94E-05	-4.69E-10	-1.39E-14	9.06E-19
3.35714	2.83321	5.19E-05	-6.25E-10	-1.73E-14	1.13E-18
3.42857	2.84776	6.45E-05	-7.80E-10	-2.06E-14	1.36E-18
3.5	2.86232	7.71E-05	-9.36E-10	-2.40E-14	1.59E-18
3.57143	2.87688	8.96E-05	-1.09E-09	-2.74E-14	1.81E-18
3.64286	2.89144	1.02E-04	-1.25E-09	-3.08E-14	2.04E-18
3.71429	2.90599	1.15E-04	-1.40E-09	-3.41E-14	2.26E-18
3.78571	2.92055	1.27E-04	-1.56E-09	-3.75E-14	2.49E-18
3.85714	2.93511	1.40E-04	-1.71E-09	-4.09E-14	2.72E-18
3.92857	2.94966	1.52E-04	-1.87E-09	-4.42E-14	2.94E-18
4	2.96422	1.65E-04	-2.03E-09	-4.76E-14	3.17E-18
4.07143	2.98517	1.69E-04	-3.99E-09	4.49E-14	2.00E-18
4.14286	3.00612	1.73E-04	-5.96E-09	1.37E-13	8.39E-19
4.21429	3.02707	1.77E-04	-7.93E-09	2.30E-13	-3.27E-19
4.28571	3.04802	1.81E-04	-9.90E-09	3.22E-13	-1.49E-18
4.35714	3.06897	1.85E-04	-1.19E-08	4.15E-13	-2.66E-18
4.42857	3.08992	1.89E-04	-1.38E-08	5.07E-13	-3.82E-18
4.5	3.11087	1.93E-04	-1.58E-08	6.00E-13	-4.99E-18
4.57143	3.08601	1.75E-04	-1.33E-08	4.99E-13	-4.01E-18
4.64286	3.06115	1.58E-04	-1.08E-08	3.99E-13	-3.04E-18
4.71429	3.03629	1.40E-04	-8.27E-09	2.98E-13	-2.06E-18
4.78571	3.01143	1.23E-04	-5.75E-09	1.98E-13	-1.08E-18
4.85714	2.98657	1.05E-04	-3.24E-09	9.71E-14	-1.04E-19
4.92857	2.96171	8.77E-05	-7.31E-10	-3.43E-15	8.73E-19
5	2.93685	7.01E-05	1.78E-09	-1.04E-13	1.85E-18

5.3 Validation of model

The predicted crack path for a hole at e = 4.5 mm is compared with experimental data points in Fig. 5.1. The predicted crack path matches reasonably well with experimental data points.

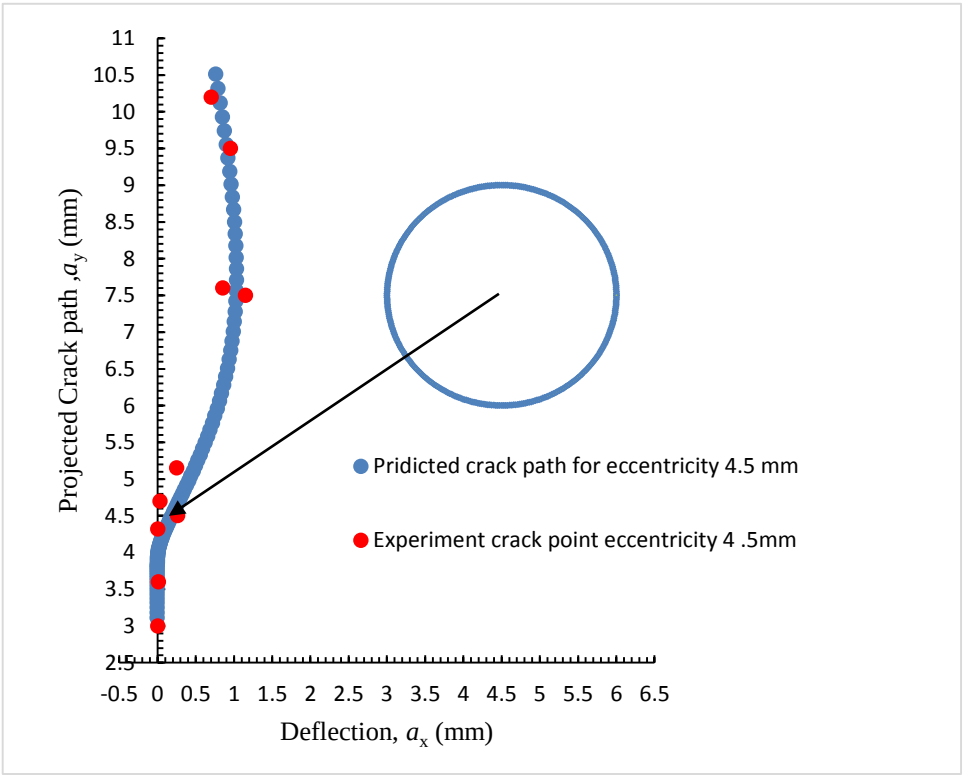

Fig. 5.1 Comparison of predicted crack length to experimental data

The fatigue projected crack length Comparison of predicted crack length (a_x) vs. experimental data with linear perfect fit for eccentricity 4.5 mm is shown in Fig. 5.2 and Comparison of predicted crack length (a_y) vs. experimental data with linear perfect fit for eccentricity 4.5 mm is shown in Fig.5.3.

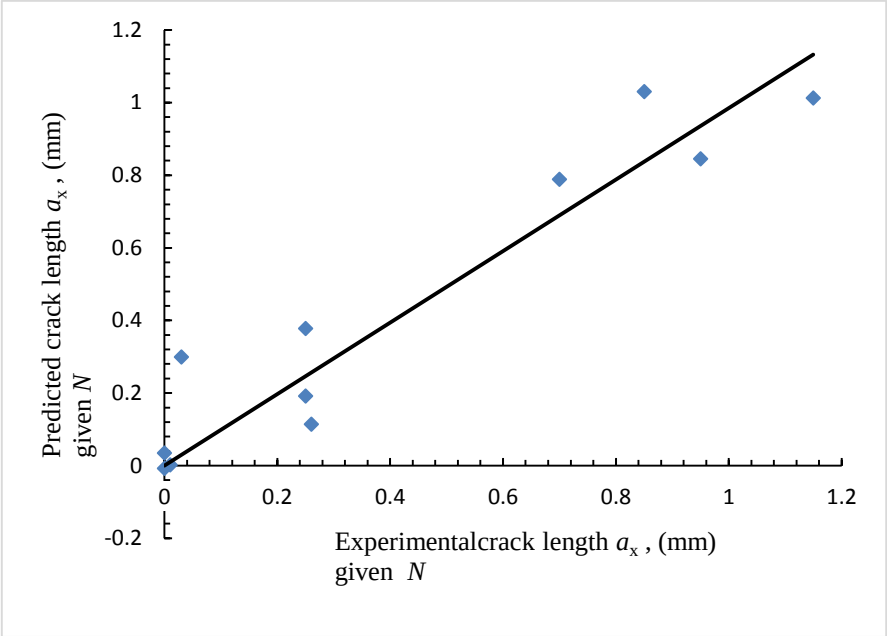

Fig. 5.2 Comparison of predicted crack length (a_x) vs. experimental data with linear perfect fit for eccentricity 4.5 mm

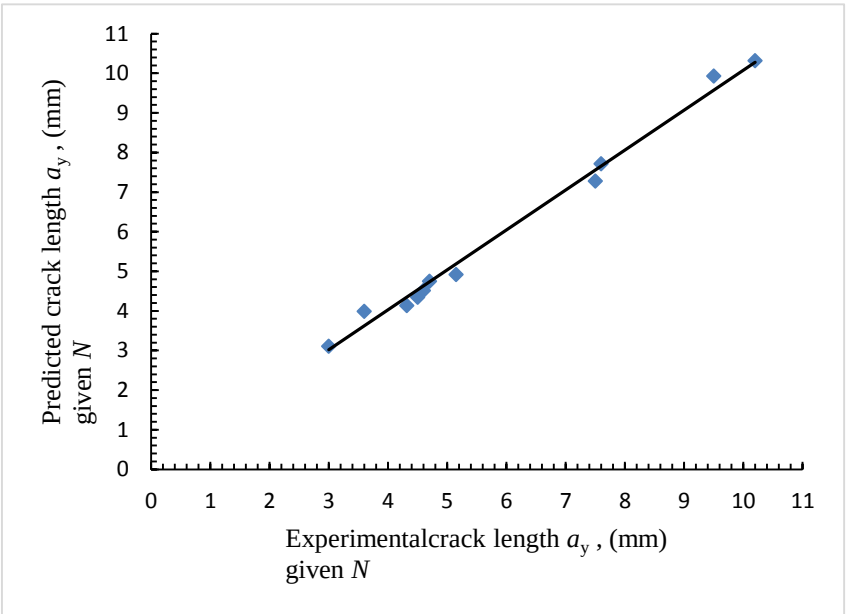

Fig. 5.3 Comparison of predicted crack length (a_y) vs. experimental data with linear perfect fit for eccentricity 4.5 mm

CHAPTER 6

Conclusions and future work

Conclusions:

1. It is observed that crack merges to the hole when eccentricities are 1.5 mm and 3 mm. Beyond 3 mm the crack deflects and the magnitude of deflection decreases with increase of eccentricity.
2. The presence of hole in the beam results in crack growth acceleration or retardation depending on the eccentricity of the hole. The eccentricity 3 mm results in maximum retardation in the present case.
3. The delay in crack propagation for eccentricity 3 mm is due to the propagation of crack through compressive stress field as has been explained by stress distribution along the crack path.
4. Gauss Amplitude model can be used to determine the fatigue crack deflection (a_x). Polynomial curve fitting can be used to determine projected crack length (a_y).
5. Using the above procedure it is possible to predict the projected crack extensions corresponding to a given number of cycles and predict crack path satisfactorily.
6. Eccentricity and diameter of the hole are two important parameters that decide crack path and crack propagation rate.

SUGGESTED FUTURE WORK

1. The proposed crack path model may be tried to predict fatigue crack path for different combinations of hole diameters and eccentricities.
2. The proposed models may be attempted for other specimen geometries.

References:

1. Varfolomeev, I., *et al*. "Fatigue crack growth rates and paths in two planar specimens under mixed mode loading." *International Journal of Fatigue* 58 (2014): 12-19.
2. Boulenouar, A., *et al*. "Two-dimensional numerical estimation of stress intensity factors and crack propagation in linear elastic analysis." *Engineering, Technology & Applied Science Research* 3.5 (2013): pp-506.
3. Miranda,A.C.O., *et al.* "Fatigue Life and Crack Path Prediction in Generic 2D Structural Components." *Engineering Fracture Mechanics* v.70 (10), p.1259-1279, 2003**.**
4. Tang, L., *et al.* "Experimental study of the strain-strengthening effect on the mixed mode notch-crack fatigue propagation in austenitic stainless steel 06Cr19Ni10." *Engineering Fracture Mechanics* 134 (2015): 54-60.
5. Tarafder, S., *et al*. "Compliance crack length relations for the four-point bend specimen." *Engineering fracture mechanics*47.6 (1994): 901-907.
6. Beden, S. M. "Review of fatigue crack propagation models for metallic components." *European Journal of Scientific Research* ISSN 1450-216X vol.28 No.3, pp.364-397, 2009.
7. Wang, G.S., *et al*. "strip model for fatigue crack growth predictions under general load conditions." *Engineering Fracture Mechanics,* v. 40, pp. 507–533, 1991.
8. Tokaji, K., *et al*. "The growth behaviour of microstructurally small fatigue cracks in metals." *Short fatigue cracks, ESIS* 13 (1992): 85-99.
9. Ming-Yuan, He., *et al*. "Crack deflection at an interface between dissimilar elastic materials." *International Journal of Solids and Structures* 25.9 (1989): 1053-1067.
10. Parmigiani, J. P., *et al*. "The roles of toughness and cohesive strength on crack deflection at interfaces." *Journal of the Mechanics and Physics of Solids* 54.2 (2006): 266-287.
11. Faber, K. T., *et al*. "Crack deflection processes-I. Theory." *Acta Metallurgica* 31.4 (1983): 565-576.
12. Rödel, J. "Interaction between crack deflection and crack bridging."*Journal of the European Ceramic Society* 10.3 (1992): 143-150.

13. Toribio, J., *et al*. "Crack paths in cold drawn pearlitic steel subjected to fatigue and fracture." *CP2009*. 2013.
14. Caron, I., *et al.* "Expanded hole method for arresting crack propagation: residual stress determination using neutron diffraction." *Physica B: Condensed Matter* 350.1 (2004): E503-E505.
15. Ghfiri, R., *et al*. "Effects of expanded and non-expanded hole on the delay of arresting crack propagation for aluminum alloys." *Materials Science and Engineering: A* 286.2 (2000): 244-249.
16. Makabe, Ch., *et al*. "Crack-growth arrest by redirecting crack growth by drilling stop holes and inserting pins into them." *Engineering Failure Analysis*16.1 (2009): 475-483.
17. Murdani, A., *et al*. "Stress concentration at stop-drilled holes and additional holes." *Engineering Failure Analysis* 15.7 (2008): 810-819.
18. Dhondt, Guido. "Application of the Finite Element Method to mixed-mode cyclic crack propagation calculations in specimens." *International Journal of Fatigue*58 (2014): 2-11.
19. Erdogan, F., *et al*. "On the crack extension in plates under plane loading and transverse shear." *Journal of Fluids Engineering* 85.4 (1963): 519-525.
20. Sih, George C. "Strain-energy-density factor applied to mixed mode crack problems." *International Journal of fracture* 10.3 (1974): 305-321.
21. Sih, George C. *Mechanics of fracture initiation and propagation: surface and volume energy density applied as failure criterion*. Vol. 11. Springer Science & Business Media, 2012.
22. Sih, G. C. "Discussion: 'Some observations on Sih's strain energy density approach for fracture prediction', by I. Finnie and HO Weiss." *International Journal of Fracture* 10.2 (1974): 279-283.
23. Theocaris, P. S., *et al*. "The T-criterion applied to ductile fracture." *International Journal of Fracture* 20.4 (1982): R125-R130.
24. Theocaris, P. S., *et al*. "Experimental study of the T-criterion in ductile fractures." *Engineering Fracture Mechanics*17.5 (1983): 439-447
25. Standard Test Methods for Tension Testing of Metallic Materials. *Annual Book of ASTM Standards*, E8/E8M-13a, 2013.